Selective anchoring groups for molecular electronic junctions with ITO electrodes

Inco J. Planje,[a†*] Ross J. Davidson,[b] Andrea Vezzoli,[a] Abdalghani Daaoub,[c] Sara Sangtarash,[cd] Hatef Sadeghi,[c] Santiago Martín,[ef] Pilar Cea,[ef] Colin J. Lambert,[d] Andrew Beeby,[b] Simon J. Higgins,[a] and Richard J. Nichols[a*]

[a] *Department of Chemistry, University of Liverpool, Crown St, Liverpool, L69 7ZD, UK*

[b] *Department of Chemistry, Durham University, South Rd, Durham, DH1 3LE, UK*

[c] *School of Engineering, University of Warwick, Coventry CV4 7AL, UK*

[d] *Department of Physics, Lancaster University, Lancaster LA1 4YW, UK*

[e] *Instituto de Nanociencia y Materiales de Aragón (INMA), Universidad de Zaragoza-CSIC, 50009 Zaragoza, Spain*

[f] *Departamento de Química Física, Facultad de Ciencias, Universidad de Zaragoza, Spain*

[†] *Present address: Department of Chemistry, King's College London, 7 Trinity Street, London SE1 1DB, UK*

** Corresponding authors: inco.planje@kcl.ac.uk, nichols@liverpool.ac.uk*

ABSTRACT

Indium tin oxide (ITO) is an attractive substrate for single-molecule electronics since it is transparent while maintaining electrical conductivity. Although it has been used before as a contacting electrode in single-molecule electrical studies, these studies have been limited to the use of carboxylic acid terminal groups for binding molecular wires to the ITO substrates. There is thus the need to investigate other anchoring groups with potential for binding effectively to ITO. With this aim, we have investigated the single-molecule conductance of a series of eight tolane or "tolane-like" molecular wires with a variety of surface binding groups. We first used gold-molecule-gold junctions to identify promising targets for ITO selectivity. We then assessed the propensity and selectively of carboxylic acid, cyanoacrylic acid, and pyridinium-squarate to bind to ITO and promote the formation of molecular heterojunctions. We found that pyridinium squarate zwitterions display excellent selectivity for binding to ITO over gold surfaces, with contact resistivity comparable to carboxylic acids. These single-

molecule experiments are complemented by surface chemical characterization with X-ray photoelectron spectroscopy, quartz crystal micro-balance, contact angle determination, and nanolithography using an atomic force miscroscope. Finally, we report the first density-functional theory calculations involving ITO electrodes to model charge transport through ITO-molecule-gold heterojunctions.

KEYWORDS: Scanning tunneling microscopy, indium tin oxide, ITO, STM break junction, STM-I(t), single-molecule conductance, anchoring groups, X-ray photoelectron spectroscopy.

This article is dedicated to the memory of Professor Nongjian Tao.

In 2007 Nongjian Tao and co-authors presented an inspiring work on the use of indium tin oxide (ITO) as a contacting electrode in single molecular electronics,[1] also highlighting its potentially attractive features in such studies. These include its optical transparency while maintaining good electrical conductivity, which is a result of the high electron doping provided by tin. Although ITO, which is an n-type degenerate semiconductor with an optical bandgap of 3.5–4.3 eV,[2-3] had been widely used for many years in photovoltaic devices and organic light-emitting diodes (OLEDs) this study by Tao and co-workers[1] was the first to demonstrate that ITO can be used to form single-molecule electrical junctions.[1] It was shown that n-alkane backbones terminated with carboxylic acid anchoring groups at each end could form molecular bridges between an ITO surface and an ITO-coated tip of a conducting AFM (c-AFM). This approach enabled defined single-molecule electrical measurements with ITO contacting electrodes using a homologous series of n-alkane dioic acids (with n = 2, 4 and 6) as molecular targets. The authors demonstrated that stable junctions could be formed, although the ITO-carboxylate binding was found to be around 7-8 times weaker than the widely deployed thiol-gold anchoring.[1] The contact conductance for ITO-carboxylate was also discovered to be less than that for gold-carboxylate contacts, although not by a large margin (425 versus 477 nS). This pioneering work by NJ Tao and co-workers paved the way for ITO as a contacting electrode in single-molecule electronics and eventually, a demonstration of single-molecule optoelectronics.

NJ Tao and co-workers also highlighted the potential advantage of ITO over conventional metal contacting electrodes such as gold,[1] since the latter quench photoexcited molecular states, opening up the possibility to deploy ITO contacting electrodes in single-molecule optoelectronic and photovoltaic devices. Although Tao did not explore this aspect in this 2007 publication, a later study by the Lindsay group did indeed use ITO as a contacting

electrode in single-molecule optoelectronic measurements.[4] They used the same carboxylate/ carboxylic acid attachment chemistry as Tao and coworkers[1] to anchor a photoactive fullerene-porphyrin dyad to the ITO surface.[4] A scanning tunneling microscope (STM) was used to contact the top of the fullerene-porphyrin dyad molecule, thereby forming ITO-fullerene/porphyrin-gold heterojunctions, with a pyridyl group anchoring to the gold STM tip. Upon illumination, through the transparent ITO, the junction conductance increased considerably, which was attributed to the formation of long-lived charge-separated states between the molecular dyad and ITO surface.[4] ITO has also been used as a material to form electrical contacts to molecular films from mesoscopic to macroscopic areas. For example, Atesci et al. have contacted self-assembled monolayers of ruthenium complexes on ITO with ITO coated c-AFM probes and phosphonic acid anchoring group (~100 molecules contacted),[5] and studied the rectifying properties of the resulting junctions.

Beyond the two publications mentioned above,[1, 4] to the best of our knowledge, there appears to have been no further development of ITO as a contacting electrode for forming *single-molecule* electrical junctions. This lack of development is perhaps surprising given the continued interest in ITO and other transparent conductive electrodes in photovoltaic and OLED devices. In addition, within the field of molecular electronics there has also been a continued interest in the optical modulation of electrical devices. This interest is also complemented by using ITO as a gate material in high-performance CMOS transistors, where it has been deployed in channel thickness down to 1 nm.[6] It is noteworthy that ITO has featured strongly in sensor and electrochemical applications, so electron transfer at ITO-molecule interfaces (see, *e.g.* the work performed by Gooding *et al.*[7]) is a theme of continuing contemporary attention. These collected interest areas for ITO highlight the further need to develop it as a contacting electrode in nanoscale electronic junctions or fundamental studies of electron transport at ITO-molecule interfaces. This is the subject of the present work, which examines several new anchoring groups for binding to ITO for the formation of nanoscale electronic junctions.[5]

Although there has been substantial work on developing large-area molecular monolayers on ITO,[8-13] for example phosphonic acids and amino silanes, in the case of single-molecule electrical junctions to ITO, the interface chemistry has not been extended beyond carboxylic acids. In this present study, non-symmetric tolane or “tolane-like” molecular wires with novel surface binding groups are used to form molecular junctions between an ITO surface and a gold tip. An STM is used to monitor the stochastic formation of these ITO-molecule-gold heterojunctions by measuring telegraphic tunneling current signals with the so-called current-time (*I*-*t*) technique.[14-15] Binding to the top gold electrode is favorably achieved through gold-sulfur linkages. Surface characterization is performed with X-ray photoelectron

spectroscopy (XPS), quartz crystal microbalance, contact angle measurements, and atomic force microscopy (AFM) nanolithographic carving. These collective results highlight that pyridinium squarate is a favorable new group for selectively forming contacts to ITO. The study concludes with the presentation of new theoretical modeling of single-molecule electrical junctions with ITO contacting electrodes, which is challenging given the chemical and physical heterogeneity of such substrates.

RESULTS AND DISCUSSION

Current-distance screening using gold substrates

One of the key aspects we considered for choosing the anchoring groups is their ability to selectively bind to transparent electrodes such as ITO. This section describes our initial screening of new anchoring groups using gold substrates before we move onto ITO substrates in following sections. Here, in this first part we used the STM break-junction (STM-BJ) technique[16] to assess the conductance of a set of molecular wires and their behavior in gold-molecule-gold junctions. For this, we screen a variety of molecular wires all containing a tolane (diphenylacetylene) or "tolane-like" backbone, which is a well-studied archetypal molecular wire.[17-19] Our envisioned experimental measurement procedures, described in following sections, entails molecules selectively bound to an ITO substrate through one anchoring group, and contacted by a gold STM tip to complete the ITO-molecule-gold molecular junction. The successful molecules therefore require distinct anchoring groups that allow for selective binding to ITO at one end, and the gold STM tip at the other. To assess the selectivity of binding groups to gold the initial screening was carried out for compounds shown in Figure 1 using the STM-BJ method on gold substrates. Should the binding groups proposed for ITO contacting electrodes also give rise to the formation of good gold-molecule-gold junctions there would be little chance of selective binding in the subsequent ITO-molecule-gold junctions.

As described above, each of the molecular wires has on one side a well-studied sulfur anchoring group for binding to gold and on the other with an anchoring group designed for ITO. Figure 1 presents the workflow used in this project, with the structures (top), the 2D conductance histograms for the screening experiments with gold-molecule-gold homojunctions (middle panel) and then a summary of the detailed investigations made to identify the most favorable ITO surface binding (lower panel). The first two wires are dimethyldihydrobenzo[b]thiophene-tolane-carboxylic acid (**1**) and methylthio-tolane-3-pentanedione (**2**). A representative 2D conductance-distance plot of **1** shows that this molecular wire readily forms molecular junctions between two gold electrodes, and the same applies to **2**. This result indicates that the oxygen-containing anchoring groups in **1** and **2**

interact with gold, since they form good junctions and therefore, they would not have any selectivity towards ITO.

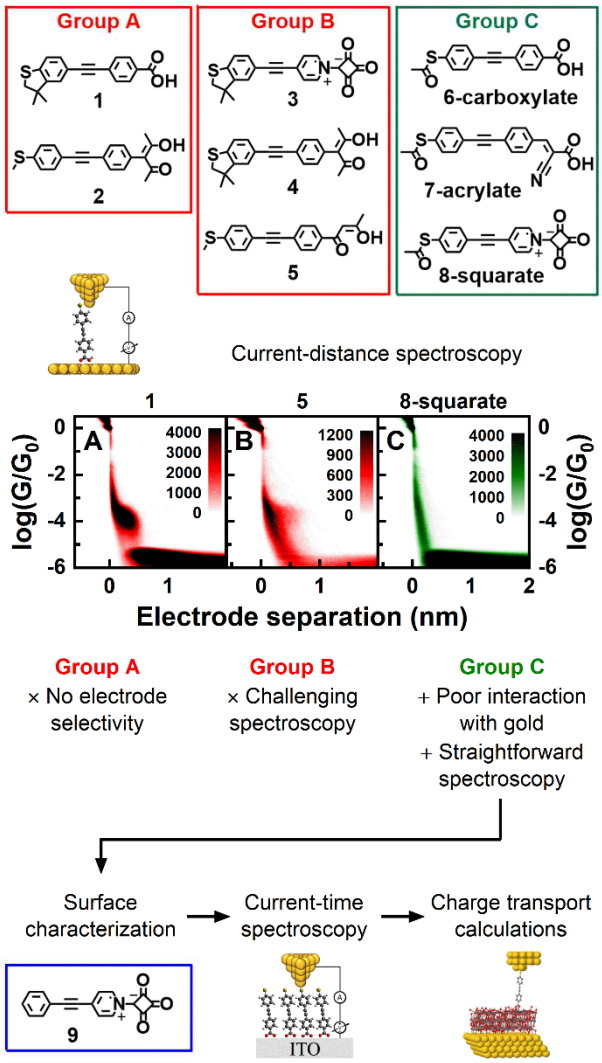

Figure 1 Workflow scheme for the project. Molecular structures (top) are divided into three groups based on results using gold-molecule-gold homojunctions. A representative 2D conductance-distance plot from each group (middle panel) highlights differences in binding to gold electrodes. The molecular wires in group C were studied further using surface characterization experiments, current-time spectroscopy and theoretical modeling (compounds **6**-**8**).

The next three wires are dimethylbenzothiophene-tolane-pyridinium-squarate (**3**), dimethylbenzothiophene-tolane-3-pentanedione (**4**), and (Z)-3-(4-((4-(methylthio)phenyl)ethynyl)phenyl)-4-oxopent-2-en-2-olate which contains a (Z)-4-oxobut-2-en-2-olate binding group (**5**). Inspiration for the pyridinium squarate group was drawn from Li et al.[20] For these squarate compounds in this study the molecular backbone cannot strictly

be called a “tolane” as they have a pyridinium ring in place of one of the phenyls, and hence they are referred to here as “tolane-like” (since like tolanes they have 2 aromatic rings connected by an acetylene linker). This group of wires shows potential for achieving controlled-orientation in heterojunctions. However, as **2** readily forms junctions between two gold electrodes and keto-enol tautomerism can complicate the surface chemistry at a metal oxide interface, either (Z)-4-oxo-pent-2-en-2-olate (in **2** or **4**) or (Z)-4-oxobut-2-en-2-olate (in **5**) can be seen as a less suitable anchoring group for ITO. Compounds **1**, **3** and **4** possess the 3,3-dimethyl-2,3-dihydrobenzo[b]thiophene (DMBT) surface binding group which has been shown as a very effective anchor for gold break junctions.[21] Although this would be very good for our single-molecule experiments it is less suited for surface characterization, on account of the bulky nature of the DMBT group which might impede self-assembly and defined molecular orientation on metallic surfaces.

The final set of wires are thio-tolane-carboxylic acid (**6-carboxylate**), thio-tolane-cyanoacrylic acid (**7-acrylate**), and thio-tolane-pyridinium-squarate (**8-squarate**), shown on the right of Figure **1** (top). In the case of **7-acrylate**, the term “acrylate” is used as an abbreviation for “cyanoacrylate”. These three compounds all have a thiol functionality (protected as thioacetate) at one terminus, which is an excellent and well-studied gold surface binding group.[22-26] All three of these wires do not readily form junctions between gold electrodes as evidenced by the 2D histograms, an example of which is shown for **8-squarate** in Figure **1** (middle panel, right). This behavior indicates that they are worthy of further investigation as candidates that might selectively orient in ITO-molecule-gold heterojunctions. Furthermore, the presence of a strong, covalent anchor such as a thiolate ensures robust self-assembly, advantageous for XPS experiments and surface characterization. These three molecular wires were therefore carried forward for further investigation.

Surface characterization

Surface characterization has been achieved with X-ray photoelectron spectroscopy (XPS), quartz crystal microbalance (QCM) and contact angle measurements. In addition, nanolithographic carving of a monolayer of molecules was performed using atomic force microscopy (AFM).

A detailed description of the XPS data for compounds **6-carboxylate**, **7-acrylate**, and **8-squarate** with gold and ITO substrates is given in the supporting information. Examination of XPS data for the sulfur 2p region is informative in assessing the assembly of the compounds onto ITO and in analyzing the relative propensities of the terminal groups to bind to either gold or ITO substrates. Illustrative XPS data for the sulfur 2p region for **8-squarate** is shown in Figure **2**. XPS characterization of self-assembled monolayers (SAMs) of **8-squarate**

shows that, upon self-assembly on a gold substrate, the S2p peaks are shifted to lower binding energy, as the molecule binds covalently to the gold surface. In the case of SAMs adsorbed onto gold substrates, the ratios between unbound and bound sulfur are 35:65 for **6-carboxylate**, 52:48 for **7-acrylate**, and 16:84 for **8-squarate**. From the XPS analysis of surface bound sulfur versus sulfur not bound to the surface (see the SI) we conclude that molecules in a SAM of **8-squarate** interact with the gold substrate predominantly via the thiol group, thereby implying relatively little gold surface binding through the pyridinium squarate group. However, the same compound self-assembled on ITO, shows no change in binding energy in the sulfur 2p region from that of the "free" molecule (measured as powder). These results highlight the non-selectivity of (substituted) carboxylic acids over thiols for binding to gold subtrates. **8-squarate**, on the other hand, displayed excellent selectivity towards ITO surfaces, since 8-squarate predominantly binds to gold through its thiol terminus.

XPS spectra have also been recorded for **8-squarate** in the N1s region. Both a SAM of **8-squarate** on ITO and the powder sample give a pair of peaks in the N1s region with similar peak energy values. This result indicates that the N atom in **8-squarate** has a similar binding environment for both the powder sample and the SAM on ITO. Therefore, it can be concluded that the N atom of the pyridinium moiety and the ITO substrate do not interact, and the adsorption on ITO occurs through the squarate. However, it is hard to extract information from the O1s region of the XPS spectra, as it is a convolution of signals associated with to the molecular wire with those arising from the high oxygen content of the substrate. Further details on the XPS measurements are presented in the SI.

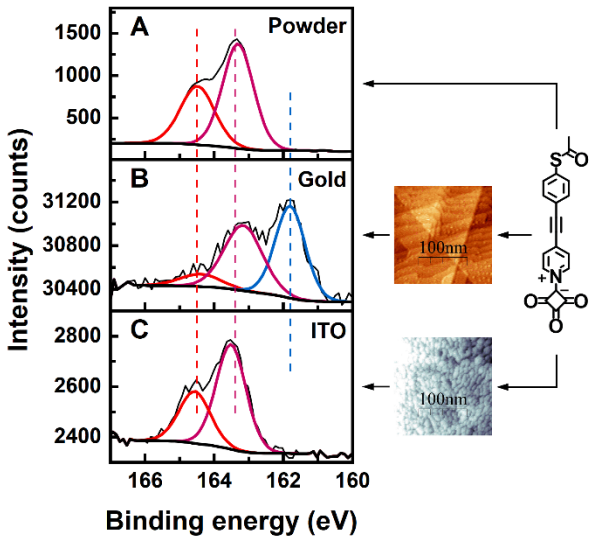

Figure 2. X-ray photoelectron spectroscopy data shows the lack of interaction between gold and the squarate group. XPS spectra in the S2p region for **8-squarate** (A) in powder, (B) adsorbed onto a gold surface, and (C) adsorbed onto an ITO surface.

We then performed quartz crystal microbalance (QCM) measurements on a “tolane-like” compound with a squarate terminal group and no thiol anchoring group (**9** in Figure **1**). A QCM resonator was incubated in a 10^{-4} M solution of **9** in THF:chloroform (1:4) and the frequency was monitored as a function of time. After 48 hours of incubation, no change in the frequency was observed, confirming the poor affinity of the pyridinium squarate group to a gold substrate.

Water contact angle measurements were carried out on gold and ITO substrates modified with **6-carboxylate**, **7-acrylate**, and **8-squarate** to confirm the specific affinity of the carboxylic acid, cyanoacrylic acid and pyridinium squarate to the ITO substrate. When ITO substrates were used to support the monolayers, angles of ca. 80º were obtained in all cases. This result indicates that all three of these monolayers expose the same terminal group pointing (*i.e.* the thiol/thioacetate) away from the ITO substrate. Meanwhile, for modified gold substrates supporting the monolayer, the angle values decrease to 70º, 72º and 63º for **6-carboxylate**, **7-acrylate**, and **8-squarate**, respectively. This finding reveals that the more hydrophilic non-sulfur groups are exposed on the top surface of the film, which agrees with the conclusions from the XPS data.

Finally, we performed nanolithographic carving of a monolayer of **6-carboxylate** on ITO using an AFM contact-mode. When we scan the surface using a high force setpoint, we observe a carved patch on the surface (see Figure S33 in the SI for details). No such change can be observed for a clean ITO substrate without a molecular layer.

Current-time spectroscopy using ITO substrates

The STM-*I*(*t*) technique was used in this study, also referred to as 'blinking'.[14-15, 27-31] This method relies on stochastic binding events where molecules bind and un-bind from the STM tip due to thermal fluctuations, resulting in switching between low and high current values. When the current is followed in the time domain it has the appearance of telegraphic noise and the technique of following the current (*I*) with time (*t*) has been therefore termed the *I*(*t*) method.[14-15] The technique can be deployed with ordered or disordered molecular monolayers, or even on a sub-monolayer of molecules adsorbed on a substrate.[14-15] This method is suitable for our study since well-ordered molecular monolayers are not a prerequisite. Nevertheless, junction formation requires adsorption of the target molecules on ITO, which has been confirmed by the surface characterization data discussed in the preceding section. The target molecules (**6-carboxylate**, **7-acrylate**, and **8-squarate**) were adsorbed onto the ITO substrate, which was then approached using a gold STM tip (Figure **3**A). As the tip is brought within sufficient distance and the STM feedback loop is turned off, abrupt changes (jumps) in the current signal indicate the stochastic formation and rupture of molecular bridges. The current signal is recorded as a function of time. Examples of such

current jumps are presented in Figure **3**C-E, where the abrupt increase in current corresponds to a molecular binding event, and a decrease corresponds to a molecular junction breaking event. Most of the jumps occur at relatively consistent values just below 1 nA, but all three systems occasionally show higher current jumps, as shown in Figure **3**F-H. We believe these jumps at higher currents arise from molecules that coordinate to the ITO surface with a different configuration (see also the theoretical discussion below). We observed no characteristic current jumps on clean ITO substrates in the absence of molecules.

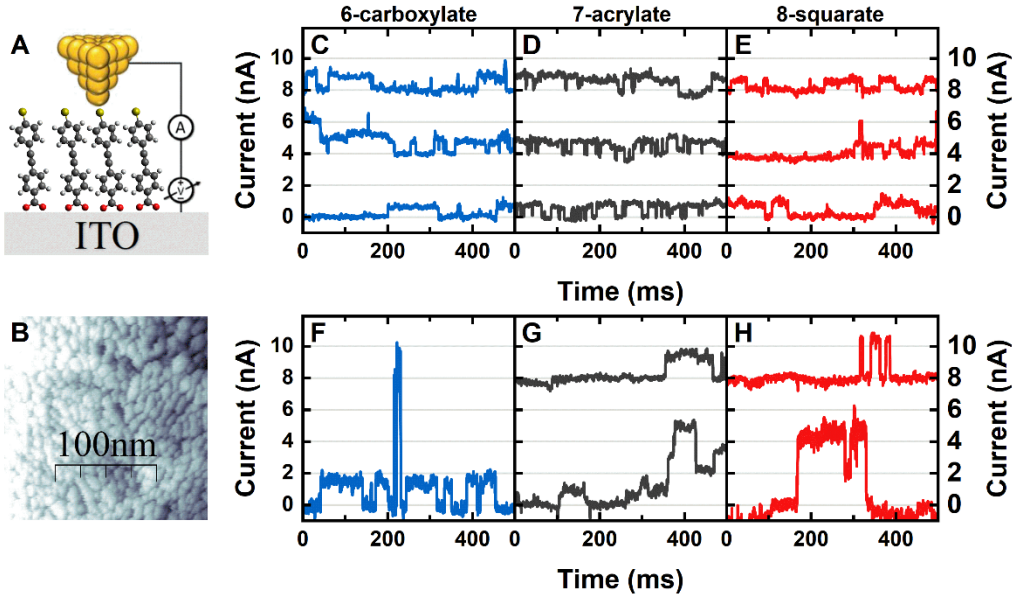

Figure 3 Individual traces for ITO-molecule-gold junctions show current jumps, confirming the stochastic formation of single-molecule junctions. (A) Schematic setup for the current-time spectroscopy experiment with compound **6-carboxylate** as an example. (B) STM image showing the clean ITO surface. (C-E) Example traces showing jumps at the *average* current of all traces in each dataset. (F-H) Example traces showing jumps at *higher* current values, which occur less frequently. Traces are offset for clarity, and all measurements were carried out using a negative sample bias of 100 mV.

Traces comprising hundreds of individual "jumps" were compiled into conductance histograms. One-dimensional histograms were compiled from the raw traces and provide counts for the most probable average conductance values of these junctions, (Figure 4A-C). The raw traces were further analyzed using an automated Python algorithm,[32-33] where each trace was sliced between jumps using the second derivative of the current signal. These slices were compiled in 2D density maps (Figure 4D-F), providing insight into the temporal stability of the molecular heterojunctions. Since these 2D maps only contain the current

jumps, there is no observed background as is the case for the 1D histograms. Details about data collection and analysis are provided in the supporting information. Overall, the average junction conductance values are 7.1 nS for **6-carboxylate**, 4.6 nS for **7-acrylate**, and 5.6 nS for **8-squarate** (Figure **4** A-C). Temporal stability plots (Figure **4** D-F) show that the junctions with pyridinium squarate also show the greatest longevity with junctions persisting for up to ~100 mS under our measurement conditions.

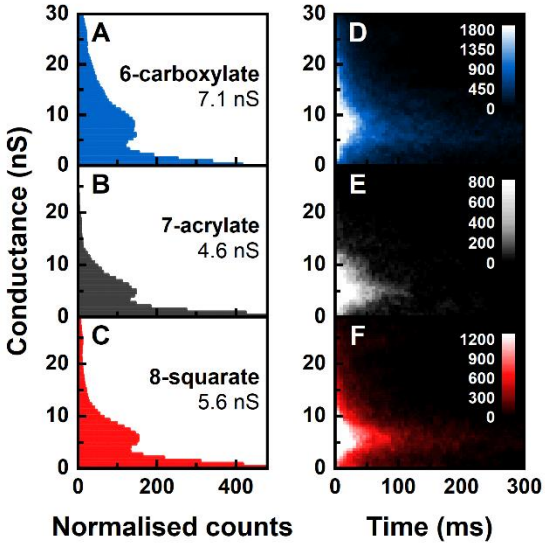

Figure 4 Histograms built from the single traces show that average junction conductance values and temporal stability is comparable for all three molecules. (A-C) One-dimensional conductance histograms for **6-carboxylate** in blue (207.5 seconds total), **7-acrylate** in gray (97 seconds total), and **8-squarate** in red (173.5 seconds total). (D-F) Two-dimensional conductance histograms for **6-carboxylate** in blue (1863 jumps out of 3106 slices), **7-acrylate** in grey (807 jumps out of 1615 slices), and **8-squarate** in red (1266 jumps out of 2559 slices). All measurements were carried out using a negative sample bias of 100 mV. 1D histograms and 2D heat maps are normalized to the total number of seconds and jumps, respectively.

Charge Transport Calculations

Transport calculations for junctions that involve ITO electrodes are challenging due to the complexity of the crystal lattice. We started by modeling the ITO electrode, using an indium oxide cubic lattice substituting cationic sites with Sn using an Sn/In ratio of 0.16.[34-37] We then used density functional theory to find an optimized structure of ITO on the gold (see methods). Next, we placed the molecules between ITO and gold electrodes and then find the optimized geometry and ground-state Hamiltonian and overlap matrix elements using the SIESTA[38] implementation of DFT. These results were then combined with the Gollum[39]

implementation of the non-equilibrium Green's function method[40] to compute the transmission coefficient of the systems (see further details in the SI). To find a suitable configuration for the formation of junctions with an ITO electrode, two different bonding structures including COO^- and COOH (H-bonding) on metal oxide surfaces were investigated, as shown in Figure S34 in the SI. The DFT results show that the COO^- structure has a higher binding energy (as shown in Table S1). Figure **5**A illustrates an example that has a fully relaxed geometry of the molecular structure in the junction with **8-squarate** anchoring to ITO. Our calculations indicate that **8-squarate** interacts with ITO through hydrogen bonding and electrostatic interactions (see Figure S39).

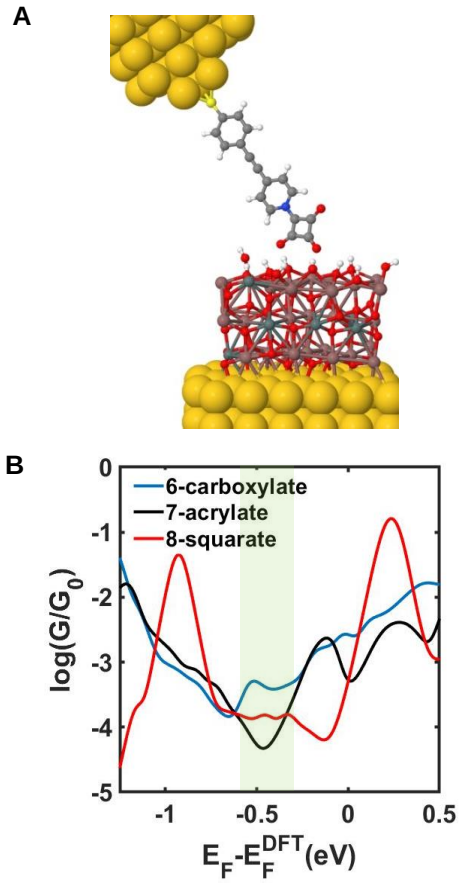

Figure 5 Calculated transmission plots of the ITO-molecule-gold junctions compare well with the experimental results. (A) Relaxed structure of **8-squarate** between gold and ITO (see the SI for the relaxed structures of all the systems). (B) Calculated electrical conductance curves versus electrode energy.

Figure **5**B shows the electrical conductance values of the molecules **6-carboxylate, 7-acrylate** and **8-square** for configurations shown in Figure S35. Typically, the Fermi energy, E_F, lies near the middle of the HOMO-LUMO gap, and comparing with the experimental

trend, our results suggest that E_F falls within the highlighted region in the figure. The calculation with three different binding configurations to electrodes for each molecule (Figure S36 and S37) indicates that electron transport through the junctions varies according to the different configurations. However, the overall trend for the average conductance over these different configurations (**6-carboxylate** > **8-squarate** > **7-acrylate)** is the same as we found in our experiments. This shows that in spite of the complexity of incorporating the doped oxide semiconductor, our calculations are in good agreement with experiment.

CONCLUSIONS

We have measured electrical transport properties of a series of tolane or "tolane-like" wires using STM techniques to form metal-molecule-metal junctions. The conductance of these molecular wires with different surface binding groups was first screened using gold pair homojunctions (gold substrates and gold STM tips, respectively) and the break-junction technique. All these molecular wires have different binding group combinations on their respective termini. Single-molecule conductance values were around $10^{-3.5}$ G_0 for all wires that formed junctions, which is slightly lower than values for tolane wires which have identical anchoring groups on their respective ends.[17] Crucially, the pyridinium squarate group does not form junctions using only gold electrodes, making it a promising candidate as a selective ITO binding group. Bearing in mind these findings for gold-molecule-gold homojunctions we then turned to ITO-molecule-gold heterojunctions, choosing the thiol anchoring group as a favorable gold binding group for the top contact to the gold STM tip. Here, we have shown the controlled orientation of the molecules by the design of their electrode-specific anchoring groups, which is confirmed by surface characterization experiments. The heterojunctions formed using current-time spectroscopy have reproducible conductance values. The selective binding of **8-squarate** to an ITO surface offers perspectives for studies where controlled orientation is required in heterojunctions. Possible directions might include future work with junction illumination through the transparent ITO electrode contacts. Further development could include ITO-molecule-ITO homojunctions employing pyridinium squarate surface anchoring and ITO-coated STM tips.

AUTHOR CONTRIBUTIONS

RJD, AB, and RJN designed the project in consultation with other team members. IJP carried out all STM experiments. AV supervised/provided training on the STM. IJP and AV analyzed all the conductance data. SM and PC carried out and analyzed all surface characterization experiments. AD, SS, and HS performed all theoretical calculations in

consultation with CJL. RJD synthesized and characterized all compounds in consultation with AB. Contributions to the manuscript writing: introduction and discussion of STM and conductance data and general discussion (IJP and RJN), synthesis (RJD), theory (SS), XPS and surface characterization (SM), with further contributions in editing from CJL, AV, SJH and PC. All authors have approved submission.

ACKNOWLEDGMENTS

This work was supported by EPSRC under grants EP/M005046/1 (Single-Molecule Photo-Spintronics, Liverpool), EP/M029522/1 (Single Molecule Plasmoelectronics, Liverpool), EP/M029204/1 (Single Molecule Plasmoelectronics, Durham), EP/N017188/1, EP/M014452/1, EP/P027156/1 and EP/N03337X/1. Support from the European Commission is provided by the FET Open project 767187 – QuIET. AV acknowledges funding from the Royal Society (URF\R1\191241) and thanks Dr. Richard J. Brooke and Prof. Walther Schwarzacher for assistance in developing the Python script used for data processing. IJP would like to thank Vivien Walter for his help with coding some of the data analysis procedures. SS thanks the Leverhulme Trust for funding (Early Career Fellowship ECF-2018-375). HS thanks UKRI for funding (Future Leaders Fellowship MR/S015329/2). SM and PC acknowledge financial assistance from Ministerio de Ciencia e Innovación from Spain and fondos FEDER in the framework of projects MAT2016-78257-R and PID2019-105881RB-I00 and support from Gobierno de Aragón through the grant numbers LMP33-18 and E31_20R with European Social Fund (Construyendo Europa desde Aragón).

Data collected using EPSRC funding at Liverpool are archived at http://datacat.liverpool.ac.uk/id/eprint/1165

Supporting Information Available: The following files are available free of charge at ***Insert Link Here***.

Synthesis, STM break-junction details, UV-VIS for scissor corrections, XPS, QCM, STM current-time setup & analysis details, AFM nanolithographic carving, binding energy and transport calculation for gold-gold electrode, method for DFT and transport calculations (PDF).

REFERENCES

1. Chen, F.; Huang, Z. F.; Tao, N. J., Forming single molecular junctions between indium tin oxide electrodes. *Applied Physics Letters* **2007,** *91* (16).

2. Hamberg, I.; Granqvist, C. G.; Berggren, K. F.; Sernelius, B. E.; Engström, L., Band-gap widening in heavily Sn-doped In_2O_3. *Physical Review B* **1984,** *30* (6), 3240-3249.
3. Yu, Z.; Perera, I. R.; Daeneke, T.; Makuta, S.; Tachibana, Y.; Jasieniak, J. J.; Mishra, A.; Bäuerle, P.; Spiccia, L.; Bach, U., Indium tin oxide as a semiconductor material in efficient p-type dye-sensitized solar cells. *NPG Asia Materials* **2016,** *8* (9), e305-e305.
4. Battacharyya, S.; Kibel, A.; Kodis, G.; Liddell, P. A.; Gervaldo, M.; Gust, D.; Lindsay, S., Optical Modulation of Molecular Conductance. *Nano Lett.* **2011,** *11* (7), 2709-2714.
5. Atesci, H.; Kaliginedi, V.; Celis Gil, J. A.; Ozawa, H.; Thijssen, J. M.; Broekmann, P.; Haga, M.-a.; van der Molen, S. J., Humidity-controlled rectification switching in ruthenium-complex molecular junctions. *Nature Nanotechnology* **2018,** *13* (2), 117-121.
6. Si, M.; Andler, J.; Lyu, X.; Niu, C.; Datta, S.; Agrawal, R.; Ye, P. D., Indium–Tin-Oxide Transistors with One Nanometer Thick Channel and Ferroelectric Gating. *ACS Nano* **2020**.
7. Chen, X.; Cheng, X. Y.; Gooding, J. J., Detection of Trace Nitroaromatic Isomers Using Indium Tin Oxide Electrodes Modified Using beta-Cyclodextrin and Silver Nanoparticles. *Analytical Chemistry* **2012,** *84* (20), 8557-8563.
8. Koh, S. E.; McDonald, K. D.; Holt, D. H.; Dulcey, C. S.; Chaney, J. A.; Pehrsson, P. E., Phenylphosphonic Acid Functionalization of Indium Tin Oxide: Surface Chemistry and Work Functions. *Langmuir* **2006,** *22* (14), 6249-6255.
9. Paniagua, S. A.; Hotchkiss, P. J.; Jones, S. C.; Marder, S. R.; Mudalige, A.; Marrikar, F. S.; Pemberton, J. E.; Armstrong, N. R., Phosphonic Acid Modification of Indium−Tin Oxide Electrodes: Combined XPS/UPS/Contact Angle Studies. *The Journal of Physical Chemistry C* **2008,** *112* (21), 7809-7817.
10. Sergani, S.; Furmansky, Y.; Visoly-Fisher, I., Metal-free molecular junctions on ITO via amino-silane binding—towards optoelectronic molecular junctions. *Nanotechnology* **2013,** *24* (45), 455204.
11. Benneckendorf, F. S.; Hillebrandt, S.; Ullrich, F.; Rohnacher, V.; Hietzschold, S.; Jänsch, D.; Freudenberg, J.; Beck, S.; Mankel, E.; Jaegermann, W.; Pucci, A.; Bunz, U. H. F.; Müllen, K., Structure–Property Relationship of Phenylene-Based Self-Assembled Monolayers for Record Low Work Function of Indium Tin Oxide. *The Journal of Physical Chemistry Letters* **2018,** *9* (13), 3731-3737.
12. Chen, X.; Luais, E.; Darwish, N.; Ciampi, S.; Thordarson, P.; Gooding, J. J., Studies on the Effect of Solvents on Self-Assembled Monolayers Formed from Organophosphonic Acids on Indium Tin Oxide. *Langmuir* **2012,** *28* (25), 9487-9495.
13. Chockalingam, M.; Darwish, N.; Le Saux, G.; Gooding, J. J., Importance of the Indium Tin Oxide Substrate on the Quality of Self-Assembled Monolayers Formed from Organophosphonic Acids. *Langmuir* **2011,** *27* (6), 2545-2552.
14. Haiss, W.; Nichols, R. J.; van Zalinge, H.; Higgins, S. J.; Bethell, D.; Schiffrin, D. J., Measurement of single molecule conductivity using the spontaneous formation of molecular wires. *Physical Chemistry Chemical Physics* **2004,** *6* (17), 4330-4337.
15. Haiss, W.; Wang, C. S.; Grace, I.; Batsanov, A. S.; Schiffrin, D. J.; Higgins, S. J.; Bryce, M. R.; Lambert, C. J.; Nichols, R. J., Precision control of single-molecule electrical junctions. *Nature Materials* **2006,** *5* (12), 995-1002.
16. Xu, B.; Tao, N. J., Measurement of Single-Molecule Resistance by Repeated Formation of Molecular Junctions. *Science* **2003,** *301* (5637), 1221-1223.
17. Hong, W.; Manrique, D. Z.; Moreno-García, P.; Gulcur, M.; Mishchenko, A.; Lambert, C. J.; Bryce, M. R.; Wandlowski, T., Single Molecular Conductance of Tolanes: Experimental

and Theoretical Study on the Junction Evolution Dependent on the Anchoring Group. *Journal of the American Chemical Society* **2012,** *134* (4), 2292-2304.
18. Yoshida, K.; Pobelov, I. V.; Manrique, D. Z.; Pope, T.; Mészáros, G.; Gulcur, M.; Bryce, M. R.; Lambert, C. J.; Wandlowski, T., Correlation of breaking forces, conductances and geometries of molecular junctions. *Scientific Reports* **2015,** *5* (1), 9002.
19. Tang, Z.; Hou, S.; Wu, Q.; Tan, Z.; Zheng, J.; Li, R.; Liu, J.; Yang, Y.; Sadeghi, H.; Shi, J.; Grace, I.; Lambert, C. J.; Hong, W., Solvent-molecule interaction induced gating of charge transport through single-molecule junctions. *Science Bulletin* **2020,** *65* (11), 944-950.
20. Li, T.-Y.; Su, C.; Akula, S. B.; Sun, W.-G.; Chien, H.-M.; Li, W.-R., New Pyridinium Ylide Dyes for Dye Sensitized Solar Cell Applications. *Organic Letters* **2016,** *18* (14), 3386-3389.
21. Kaliginedi, V.; V. Rudnev, A.; Moreno-García, P.; Baghernejad, M.; Huang, C.; Hong, W.; Wandlowski, T., Promising anchoring groups for single-molecule conductance measurements. *Physical Chemistry Chemical Physics* **2014,** *16* (43), 23529-23539.
22. Reed, M. A.; Zhou, C.; Muller, C. J.; Burgin, T. P.; Tour, J. M., Conductance of a Molecular Junction. *Science* **1997,** *278* (5336), 252-254.
23. Xiao; Xu; Tao, N. J., Measurement of Single Molecule Conductance: Benzenedithiol and Benzenedimethanethiol. *Nano Lett.* **2004,** *4* (2), 267-271.
24. Haiss, W.; van Zalinge, H.; Higgins, S. J.; Bethell, D.; Höbenreich, H.; Schiffrin, D. J.; Nichols, R. J., Redox State Dependence of Single Molecule Conductivity. *Journal of the American Chemical Society* **2003,** *125* (50), 15294-15295.
25. Li, C.; Pobelov, I.; Wandlowski, T.; Bagrets, A.; Arnold, A.; Evers, F., Charge Transport in Single Au | Alkanedithiol | Au Junctions: Coordination Geometries and Conformational Degrees of Freedom. *Journal of the American Chemical Society* **2008,** *130* (1), 318-326.
26. Leary, E.; La Rosa, A.; González, M. T.; Rubio-Bollinger, G.; Agraït, N.; Martín, N., Incorporating single molecules into electrical circuits. The role of the chemical anchoring group. *Chemical Society Reviews* **2015,** *44* (4), 920-942.
27. Chang, S. A.; He, J.; Lin, L. S.; Zhang, P. M.; Liang, F.; Young, M.; Huang, S.; Lindsay, S., Tunnel conductance of Watson-Crick nucleoside-base pairs from telegraph noise. *Nanotechnology* **2009,** *20* (18).
28. Diez-Perez, I.; Hihath, J.; Lee, Y.; Yu, L. P.; Adamska, L.; Kozhushner, M. A.; Oleynik, II; Tao, N. J., Rectification and stability of a single molecular diode with controlled orientation. *Nature Chemistry* **2009,** *1* (8), 635-641.
29. Huang, S.; He, J.; Chang, S. A.; Zhang, P. M.; Liang, F.; Li, S. Q.; Tuchband, M.; Fuhrmann, A.; Ros, R.; Lindsay, S., Identifying single bases in a DNA oligomer with electron tunnelling. *Nature Nanotechnology* **2010,** *5* (12), 868-873.
30. Pla-Vilanova, P.; Aragones, A. C.; Ciampi, S.; Sanz, F.; Darwish, N.; Diez-Perez, I., The spontaneous formation of single-molecule junctions via terminal alkynes. *Nanotechnology* **2015,** *26* (38).
31. Aragones, A. C.; Haworth, N. L.; Darwish, N.; Ciampi, S.; Bloomfield, N. J.; Wallace, G. G.; Diez-Perez, I.; Coote, M. L., Electrostatic catalysis of a Diels-Alder reaction. *Nature* **2016,** *531* (7592), 88-91.
32. Vezzoli, A.; Brooke, R. J.; Higgins, S. J.; Schwarzacher, W.; Nichols, R. J., Single-Molecule Photocurrent at a Metal–Molecule–Semiconductor Junction. *Nano Lett.* **2017,** *17* (11), 6702-6707.
33. Vezzoli, A.; Brooke, R. J.; Ferri, N.; Higgins, S. J.; Schwarzacher, W.; Nichols, R. J., Single-Molecule Transport at a Rectifying GaAs Contact. *Nano Lett.* **2017,** *17* (2), 1109-1115.

34. Paramonov, P. B.; Paniagua, S. A.; Hotchkiss, P. J.; Jones, S. C.; Armstrong, N. R.; Marder, S. R.; Brédas, J.-L., Theoretical Characterization of the Indium Tin Oxide Surface and of Its Binding Sites for Adsorption of Phosphonic Acid Monolayers. *Chemistry of Materials* **2008,** *20* (16), 5131-5133.
35. Kugler, T.; Johansson, A.; Dalsegg, I.; Gelius, U.; Salaneck, W. R., Electronic and chemical structure of conjugated polymer surfaces and interfaces: applications in polymer-based light-emitting devices. *Synthetic Metals* **1997,** *91* (1-3), 143-146.
36. Christou, V.; Etchells, M.; Renault, O.; Dobson, P. J.; Salata, O. V.; Beamson, G.; Egdell, R. G., High resolution x-ray photoemission study of plasma oxidation of indium-tin-oxide thin film surfaces. *Journal of Applied Physics* **2000,** *88* (9), 5180-5187.
37. You, Z. Z.; Dong, J. Y., Surface properties of treated ITO anodes for organic light-emitting devices. *Applied Surface Science* **2005,** *249* (1-4), 271-276.
38. Soler, J. M.; Artacho, E.; Gale, J. D.; García, A.; Junquera, J.; Ordejón, P.; Sánchez-Portal, D., The SIESTA method forab initioorder-Nmaterials simulation. *Journal of Physics: Condensed Matter* **2002,** *14* (11), 2745-2779.
39. Ferrer, J.; Lambert, C. J.; García-Suárez, V. M.; Manrique, D. Z.; Visontai, D.; Oroszlany, L.; Rodríguez-Ferradás, R.; Grace, I.; Bailey, S. W. D.; Gillemot, K.; Sadeghi, H.; Algharagholy, L. A., GOLLUM: a next-generation simulation tool for electron, thermal and spin transport. *New Journal of Physics* **2014,** *16* (9), 093029.
40. Sadeghi, H., Theory of electron, phonon and spin transport in nanoscale quantum devices. *Nanotechnology* **2018,** *29* (37), 373001.

For TOC only.

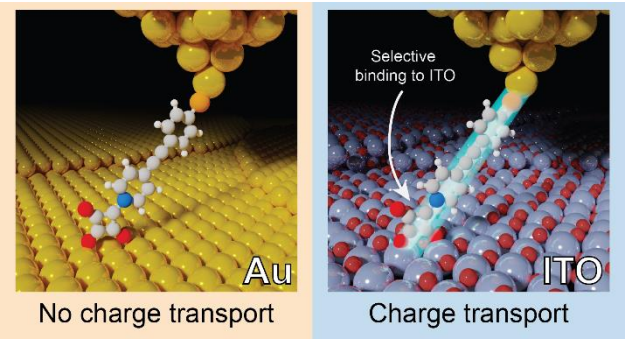
Au
No charge transport
Selective
binding to ITO
ITO
Charge transport